

Lawrence Berkeley National Laboratory

Recent Work

Title

Transcriptomic atlas of mushroom development reveals conserved genes behind complex multicellularity in fungi.

Permalink

<https://escholarship.org/uc/item/1fq6r2jp>

Journal

Proceedings of the National Academy of Sciences of the United States of America, 116(15)

ISSN

0027-8424

Authors

Krizsán, Krisztina
Almási, Éva
Merényi, Zsolt
[et al.](#)

Publication Date

2019-04-01

DOI

10.1073/pnas.1817822116

Peer reviewed

1 Transcriptomic atlas of mushroom development highlights an 2 independent origin of complex multicellularity

3 Krisztina Krizsán¹, Éva Almási¹, Zsolt Merényi¹, Neha Sahu¹, Máté Virágh¹, Tamás Kószó¹,
4 Stephen Mondo², Brigitta Kiss¹, Balázs Bálint^{1,3}, Ursula Kües⁴, Kerrie Barry², Judit Cseklye³
5 Botond Hegedűs^{1,5}, Bernard Henrissat⁶, Jenifer Johnson², Anna Lipzen², Robin A. Ohm⁷, István
6 Nagy³, Jasmyn Pangilinan², Juying Yan², Yi Xiong², Igor V. Grigoriev², David S. Hibbett⁸, László
7 G. Nagy^{1*}

8
9

10 *1 Synthetic and Systems Biology Unit, Institute of Biochemistry, BRC-HAS, Szeged, 6726,*
11 *Hungary.*

12 *2 US Department of Energy (DOE) Joint Genome Institute, Walnut Creek, CA, 94598, United*
13 *States.*

14 *3 Seqomics Ltd. Mórahalom, Mórahalom 6782, Hungary*

15 *4 Division of Molecular Wood Biotechnology and Technical Mycology, Büsgen-Institute,*
16 *University of Göttingen, Göttingen, Germany.*

17 *5 Institute of Biophysics, BRC-HAS, Szeged, 6726, Hungary.*

18 *6 Architecture et Fonction des Macromolécules Biologiques (AFMB), UMR 7257 CNRS*
19 *Université Aix-Marseille, 13288, Marseille, France.*

20 *7 Department of Biology, Microbiology, Utrecht University, 3584 Utrecht, The Netherlands*

21 *8 Biology Department, Clark University, 01610 Worcester MA, USA*

22
23

24 *To whom correspondence should be addressed: lnagy@fun genomelab.com

25
26

27 **We constructed a reference atlas of mushroom formation based on developmental**
28 **transcriptome data of six species and comparisons of >200 whole genomes, to elucidate**
29 **the core genetic program of complex multicellularity and fruiting body development in**
30 **mushroom-forming fungi (Agaricomycetes). Nearly 300 conserved gene families and >70**
31 **functional groups contained developmentally regulated genes from five to six species,**
32 **covering functions related to fungal cell wall (FCW) remodeling, targeted protein**
33 **degradation, signal transduction, adhesion and small secreted proteins (including**
34 **effector-like orphan genes). Several of these families, including F-box proteins, protein**
35 **kinases and cadherin-like proteins, showed massive expansions in Agaricomycetes, with**
36 **many convergently expanded in multicellular plants and/or animals too, reflecting broad**
37 **genetic convergence among independently evolved complex multicellular lineages. This**
38 **study provides a novel entry point to studying mushroom development and complex**
39 **multicellularity in one of the largest clades of complex eukaryotic organisms.**

40
41

42 Mushroom-forming fungi (Agaricomycetes, Basidiomycota) represent an independent lineage of
43 complex multicellular organisms with a unique evolutionary history compared to complex
44 animals, plants and stramenopiles. They comprise >21,000 species and originated ~350 million
45 years ago¹, approximately coinciding with the origin of tetrapods. Mushrooms have immense
46 importance in agriculture, ecology and medicine; they represent an important and sustainable
47 food source, with favorable medicinal properties (e.g. antitumor, immunomodulatory)².

48 Complex multicellular development in fungi has been subject to surprisingly few
49 studies³⁻⁶, resulting in a paucity of information on the genetic underpinnings of the independent
50 origins of complex multicellularity in fungi⁷. As complex multicellular structures, fruiting bodies
51 deploy mechanisms for hypha-to-hypha adhesion, communication, cell differentiation, defense
52 and execute a developmental program that results in a genetically determined shape and
53 size^{6,7}. Fruiting bodies shelter and protect reproductive cells and facilitate spore dispersal.
54 Uniquely, complex multicellularity in fungi comprises short-lived reproductive organs whereas in
55 animals and plants it comprises the reproducing individual. Nevertheless, fruiting bodies evolved
56 complexity levels comparable to that of simple animals, with up to 30 morphologically
57 distinguishable cell types described so far. Fruiting body development is triggered by changing
58 environmental variables (e.g. nutrient availability), and involves a transition from simple
59 multicellular hyphae to a complex multicellular fruiting body initial. The initial follows genetically
60 encoded programs to develop species-specific morphologies^{5,6}, which in the Agaricomycetes
61 ranges from simple crust-like forms (e.g. *Phanerochaete*) to the most complex toadstools (e.g.
62 *Agaricus bisporus*). Previous studies identified several developmental genes, including
63 hydrophobins⁸, defense-related proteins⁹, fungal cell wall (FCW) modifying enzymes¹⁰⁻¹³,
64 transcriptional regulators^{4,5,14} (e.g. mating genes) and light receptors¹⁵ (e.g. white collar
65 complex). It is not known, however, what genes comprise the 'core toolkit' of multicellularity and
66 development in the Agaricomycetes.

67 Here we investigate the general evolutionary and functional properties of fruiting body
68 development and assess whether mushroom-forming fungi evolved complex multicellularity via
69 unique or convergent solutions, compared to other complex lineages (e.g. plants, animals or
70 brown algae). We combine comparative analyses of developmental transcriptomes of six
71 species with comparisons of 201 whole genomes and focus on conserved developmental
72 functions and complex multicellularity.

73
74

75 **Results**

76 We obtained fruiting bodies in the laboratory or from the field and profiled gene expression in 3-
77 9 developmental stages and tissue types for *Coprinopsis cinerea* AmutBmut, *Schizophyllum*
78 *commune* H4-8, *Phanerochaete chrysosporium* RP78, *Rickenella mellea* SZMC22713 and
79 *Lentinus tigrinus* RLG9953-sp. We used data for *Armillaria ostoyae* C18/9 from our previous
80 work¹⁶. We report the *de novo* draft genome of *Rickenella mellea* (Hymenochaetales), the
81 phylogenetically most distant species from *Coprinopsis* in our dataset, spanning >200 million
82 years of evolution¹. To construct a reference atlas of mushroom development, we performed
83 poly(A)+ RNA-Seq on Illumina platforms, in triplicates (totalling to >120 libraries, Supplementary
84 Table 1). We obtained an average of 60.8 million reads per sample, of which on average 83.3%
85 mapped to the genomes (Supplementary Fig 1). For each species, the first and last

86 developmental stage sampled were vegetative mycelium and mature fruiting body at the time of
87 spore release, respectively. This spans all developmental events of fruiting bodies except
88 senescence. Because it is difficult to align intermediate developmental stages across species,
89 we identified developmentally regulated genes using an approach that removes developmental
90 stage identity from the analyses (see Methods). Using this strategy, we could recover >80% of
91 previously reported developmental genes of *Coprinopsis* (Supplementary Table 2). To more
92 broadly infer functionalities enriched in mushroom forming fungi, we analyzed Interpro domain
93 counts across 201 fungal genomes (including 104 Agaricomycetes), which revealed 631
94 significantly overrepresented domains in mushroom-forming fungi ($P < 0.01$, Fisher exact test,
95 abbreviated FET, Supplementary Table 3-4).
96

97 Dynamic reprogramming of the fungal transcriptome

98 We detected 12,003 - 17,822 expressed genes, of which 938-7,605 were developmentally
99 regulated in the six species (Fig. 1/a, Supplementary Table 5). We found 192-7,584 genes that
100 showed significant expression dynamics during fruiting body development ('FB' genes). Of
101 developmentally regulated genes 188-1,856 genes were upregulated at fruiting body initiation
102 ('FB-init' genes), which represents a transition from simple to complex multicellular organization.
103 Only *Phanerochaete chrysosporium* had more FB-init genes than FB genes, which is consistent
104 with its fruiting bodies being among the least complex types in the Agaricomycetes. The number
105 of genes significantly differentially expressed (DEG) at fruiting body initiation further suggests
106 that the transition to complex multicellularity is associated with a major reprogramming of gene
107 expression (Supplementary Fig. 2). The largest numbers of DEGs were observed in cap and gill
108 tissues in all four species with complex fruiting bodies. On the other hand, the expression
109 profiles of stipes changed little relative to primordium stages of *Armillaria*, *Lentinus* and
110 *Rickenella*, which is explained by the differentiation of the cap initial at the top of a primordial
111 stipe, as opposed to *Coprinopsis*, in which stipe and cap differentiation happens simultaneously
112 inside the fruiting body initial¹⁷. Many Gene Ontology (GO) terms were partitioned between
113 vegetative mycelium and fruiting body samples ($P < 0.05$, FET). Terms related to fungal cell wall,
114 oxidoreductase activity and carbohydrate metabolism were enriched in developmentally
115 regulated genes of all six species (Fig. 1/b, Supplementary Table 6), suggesting that cell wall
116 remodeling is a common upregulated function in fruiting bodies. Other commonly enriched
117 terms cover functions such as DNA replication, transmembrane sugar transport, ribosome,
118 membrane and lipid biosynthesis, while many other were specific to single species
119 (Supplementary Fig. 3).

120 To obtain a higher resolution of developmental events, we arranged developmentally
121 regulated genes into co-expression modules using the Short Time Series Expression Miner
122 (STEM)¹⁸. Developmentally regulated genes grouped into 28-40 modules, except
123 *Phanerochaete* which had eleven. The largest modules in all species contained genes
124 expressed at fruiting body initiation or in early primordia and genes with tissue-specific
125 expression peaks, in young fruiting body caps, gills, stipes, mature fruiting bodies and stipes or
126 caps (Fig 1/c; for further data see Supplementary Fig. 4 and Supplementary Note 1). Many
127 early-expressed modules show upregulation across multiple stages (hyphal knot, stage 1 and 2
128 primordia), suggestive of an early expression program overarching multiple primordium stages.

144 genes that show highest expression in vegetative mycelium and little or no dynamics later on. **b**,
145 wordcloud of Gene Ontology terms enriched in the developmentally regulated genes in the six
146 species. Word size corresponds to the number of species in which a term was significantly
147 enriched ($P < 0.05$, Fisher exact test). **c**, Analysis of co-expression modules in *Coprinopsis*
148 *cinerea*. Heatmap of 7475 developmentally expressed genes arranged based on module
149 assignment, with simplified expression profiles and the GO enrichment terms given for each
150 module (see also Supplementary Table 7). We graphically depict only 27 modules with >50
151 genes (refer to Supplementary Fig. 4 for the complete list and data for other species). The
152 distribution of key developmental genes is given on the right side of the heatmap. **d**,
153 Phylostratigraphic profile of developmentally regulated genes of *Coprinopsis cinerea*. Genes are
154 divided into age categories from genes shared by all cellular life (left) to species-specific genes
155 (right). The percentage of developmentally regulated genes compared to all genes in a category
156 is shown by a dashed line. Data for other species is presented in Supplementary Fig. 5. **e**,
157 UpSetR representation of gene families developmentally regulated in at least 5 species. See
158 also Supplementary Fig. 6.

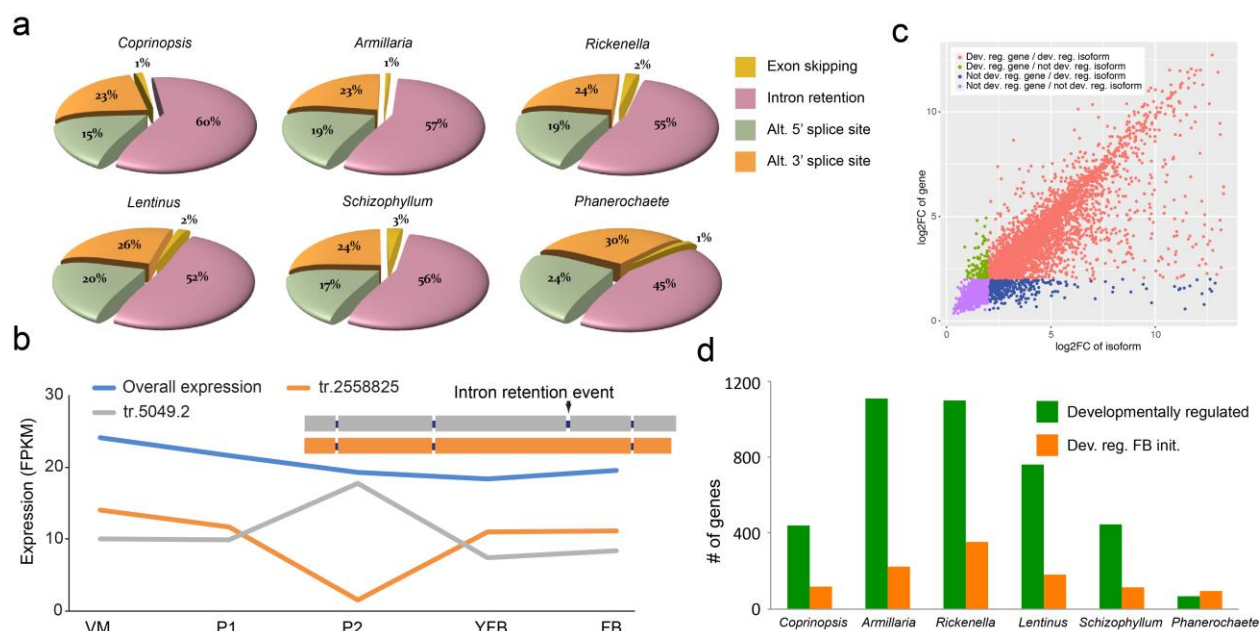
159 Most developmental gene families are older than fruiting body formation

160 We investigated the evolutionary age distribution of developmentally regulated genes using
161 phylostratigraphy¹⁹, based on a dataset of 4,483 archaeal, bacterial and eukaryotic genomes²⁰
162 supplemented with 416 fungi (of which 113 were Agaricomycetes). We assigned genes to
163 phylogenetic ages, 'phylostrata', by identifying for each gene the most phylogenetically distant
164 species in which a homolog could be detected. The phylostratigraphic profiles of all species
165 show three peaks, corresponding to two major periods of fungal gene origin: the first containing
166 genes shared by all living species, the second by the Dikarya (Ascomycota + Basidiomycota)
167 and a third containing species-specific genes. Many developmentally regulated genes have
168 homologs in simple multicellular and unicellular eukaryotes and prokaryotes: the origin of 49.3 -
169 63.3% predate the origin of mushroom-forming fungi (Fig. 1/d, Supplementary Fig. 5), indicating
170 that co-option of conserved genes contributed significantly to the evolution of fruiting bodies.
171 Nevertheless, Agaricomycetes-specific phylostrata showed a characteristic enrichment for F-
172 box genes, transcription factors and protein kinases, indicating an increased rate of origin for
173 these in mushroom-forming fungi (Supplementary Table 8).

174 Splicing patterns associate with development

175 We reconstructed transcript isoforms across developmental stages and tissue types in the six
176 species using region restricted probabilistic modeling, a strategy developed for gene-dense
177 fungal genomes²¹. We found evidence of alternative splicing for 36-46% of the expressed genes
178 (Supplementary Table 9), which is significantly higher than what was reported for fungi outside
179 the Agaricomycetes^{22,23} (1-8%). This transcript diversity was generated by 6,414 - 13,780
180 splicing events in the six species. Of the four main types of events, intron retention (44.3-60.5%)
181 was the most abundant in all species, followed by alternative 3' splice site (22.9-30.1%),
182 alternative 5' SS (15.6-24.1%) and exon skipping (0.8-2.9%) (Fig. 2/a), consistent with
183 observations made on other fungi²²⁻²⁴. No substantial difference in the proportion of spliced
184 genes and of splicing events was observed across developmental stages, tissue types or

185 species. Nevertheless, we found that several genes with nearly constant overall expression
 186 level had developmentally regulated transcript isoforms (Fig 2/b-c). The six species had 159-
 187 1,278 such genes, the highest number in *Rickenella* (1,278) and the lowest in *Phanerochaete*
 188 (159) (Fig 2/d, Supplementary Table 9). Based on their expression dynamics, these transcripts
 189 potentially also contribute to development, expanding the space of developmentally regulated
 190 genes through alternative splicing.
 191



192
 193 **Fig. 2.** Splicing patterns through fruiting body development. **a.** distribution of four main
 194 alternative splicing events across species (see also Supplementary Table 9). **b.** Genes with little
 195 dynamics can contain developmentally regulated transcripts, Schco3_2558825 is shown here
 196 as an example **c.** Scatterplot of gene versus transcript expression dynamics in *Coprinopsis*
 197 *cinerea*, highlighting developmentally regulated transcripts (red). Plotted are fold change values
 198 between the minimum and maximum expression across all developmental stages for genes (y
 199 axis) and alternative transcript (x axis). Developmentally regulated transcripts (i.e. those that
 200 show FC>4 across any two developmental stages and FPKM>4) of non-developmentally
 201 regulated genes (FC<4) are highlighted in red. **d.** bar plot of developmentally regulated
 202 transcripts that were detected within not developmentally regulated genes.

203 Conserved transcriptomic signatures of mushroom development

204 Our transcriptome data are particularly suited to detecting shared patterns of gene expression
 205 across species. We analyzed common functional signals in the six species by estimating the
 206 percent of developmentally regulated genes shared by all or subsets of the species based on
 207 Markov clustering²⁵ of protein sequences. We found 100 clusters containing developmentally
 208 regulated genes from all six species, and 196 in five species (Fig. 1/e, Supplementary Table
 209 10). These are enriched for GO terms related to oxidation-reduction processes, oxidoreductase
 210 activity, carbohydrate metabolism, among others, corresponding to a suite of carbohydrate
 211 active enzymes. Of the 100 families shared by 6 species, fifteen can be linked to the fungal cell

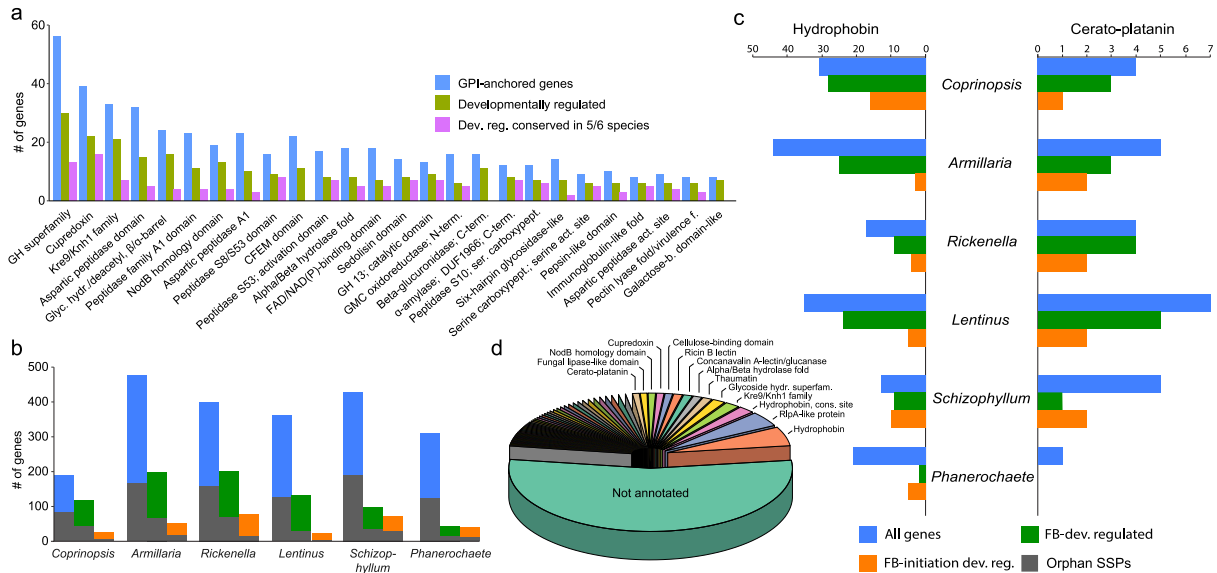
212 wall (FCW), while the remaining families cover diverse cellular functions such as
213 transmembrane transport (6 families), cytochrome p450s (5 families), targeted protein
214 degradation (5 families), or peptidases (3 families). One hundred and four gene families are
215 shared by five species excluding *Phanerochaete* (Fig 1/e), which comes as no surprise, as this
216 species produces the simple crust-like, fruiting bodies. Besides these highly conserved families,
217 an additional 73 functional groups of genes are developmentally regulated in six or five species,
218 but didn't group into gene families due to their higher rate of evolution. These include most
219 transcription factors, kinases, aquaporins, certain peptidase families and enzymes of primary
220 carbohydrate metabolism (trehalose and mannitol, Supplementary Figure 8) among others
221 (Supplementary Table 10).

222 Shared developmentally regulated gene families included a conserved suite of CAZymes
223 active on the main chitin and β -1,3- and β -1,6- glucan polymers as well as minor components of
224 the FCW. These included various glycoside hydrolases (GH), hydrophobins, expansin-like
225 proteins and cerato-platanins, among others. A large suite of β -glucanases, chitinases,
226 laccases, endo- β -1,4-mannanases, α -1,3-mannosidases were developmentally regulated, many
227 of which are also expanded in Agaricomycetes (Table 1, Supplementary Fig 7). The expression
228 of glucan-, chitin- and mannose-active enzymes is consistent with active FCW remodeling
229 during fruiting body formation and recent reports of similar genes upregulated in the fruiting
230 bodies of *Lentinula*^{12,13,26}, *Flammulina*²⁷ and *Coprinopsis*²⁸. Kre9/Knh1 homologs are
231 developmentally regulated in all species and are overrepresented in mushroom-forming fungi (P
232 = 1.45×10^{-5} , FET). This family is involved in β -glucan assembly in *Saccharomyces* and has
233 putative signaling roles through an interaction with MAP kinases²⁹. Although generally linked to
234 cellulose degradation^{30,31}, expansins, lytic polysaccharide monoxygenases and cellobiose
235 dehydrogenases have recently been shown to target chitin polymers^{32,33} or are expressed in
236 fruiting bodies of *Pycnoporus*³⁴ and *Flammulina*³⁵, suggesting a role in fruiting body
237 development. In addition, developmental expression of two alginate lyase-like families (Table 1)
238 were shared by 6 species and that of a β -glucuronidase (GH79_1) was shared by 4 species
239 (*Armillaria*, *Coprinopsis*, *Rickenella* and *Lentinus*). While the targets of these families in fruiting
240 bodies are currently unknown, their conserved expression pattern suggests roles in
241 polysaccharide metabolism during development³⁶. Comparison across 201 genomes revealed
242 that 24 of these families have undergone expansions in the Agaricomycetes (Table 1,
243 Supplementary Table 3). In summary, CAZymes might be responsible for producing fruiting
244 body-specific FCW architectures, confer adhesive properties to neighboring hyphae or plasticity
245 for growth by cell expansion. We, therefore, suggest that FCW remodeling comprises one of the
246 foundations of the transition to complex multicellularity during the life cycle of fungi.

247 A significant fraction of conserved developmentally regulated genes carry extracellular
248 secretion signals and were predicted to be glycosylphosphatidylinositol (GPI) anchored (Fig 3/a,
249 Supplementary Fig. 9). These include diverse FCW-active proteins, such as laccases (AA1),
250 glucanases (GH5, GH16, Kre9/Knh1 family), chitooligosaccharide deacetylases, but also
251 lectins, A1 aspartic peptidases and sedolisins, among others (Supplementary Table 11). GPI-
252 anchored proteins often mediate adhesion in filamentous and pathogenic fungi³⁷, but it is not
253 known whether similar mechanisms are at play in fruiting bodies⁷. Laccases and glucanases
254 could facilitate adhesion by oxidative crosslinking or other covalent modifications of neighboring
255 hyphal surfaces, although more data is needed on the biochemistry involved. Nevertheless, it

256 seems safe to conclude that FCW-active proteins may bind neighboring hyphae through
257 covalent FCW modifications in fruiting bodies, which would represent a unique adhesion
258 mechanism among complex multicellular organisms. Homologs of cadherins (adhesive proteins
259 of animals) are enriched in Agaricomycetes compared to other fungi ($P = 1.1 \times 10^{-4}$, FET) and
260 were developmentally regulated in all species. Although fewer in numbers than in animals, their
261 convergent expansion in complex multicellular fungi and metazoans could indicate recurrent co-
262 option for developmental functions.

263 Fruiting body secretomes contained a rich suite of genes encoding small secreted
264 proteins (SSPs, <300 amino acids, with extracellular secretion signal). Of the 190-477 SSPs
265 predicted in the genomes of the six species, 20-61% are developmentally regulated, with ~20%
266 being conserved across the six species (Fig. 3/b Supplementary Fig. 10). Conserved and
267 annotated genes comprise various FCW-related families, such as hydrophobins, cerato-
268 platanins, cupredoxins, lectins, Kre9/Knh1, GH12 and LysM domain proteins, among others
269 (Fig. 3/c, Supplementary Fig. 11). Hydrophobins and cerato-platanins are SSPs that self-
270 assemble into a rodlet layer on the cell surface, confer hydrophobic surfaces to hyphae that
271 hinder soaking of fruiting bodies with water. They are hypothesized to mediate adhesion, the
272 aeration of fruiting bodies^{8,38}, or pathogenicity³⁹. As reported previously⁸, most hydrophobin
273 genes are developmentally regulated (Fig. 3/d) and the family is overrepresented in the
274 genomes of mushroom-forming fungi ($P < 10^{-300}$, FET). Cerato-platanins are also expanded ($P =$
275 1.56×10^{-50} , FET) and developmentally regulated (except in *Phanerochaete*). In addition to
276 conserved genes, >40% of developmentally regulated SSPs had no functional annotations
277 and/or were species-specific orphans (Fig. 3/c). This proportion is similar to that observed in
278 ectomycorrhiza-induced SSPs^{1,40} and suggests that species-specific secreted proteins have a
279 role also in fruiting body development. Although their function in fruiting bodies is not known,
280 their role in signaling across partners in ectomycorrhizal⁴⁰ and pathogenic interactions⁴¹, or
281 within species^{42,43}, raises the possibility that some of the detected SSPs might act as fruiting
282 body effectors. This could also explain the rich SSP repertoires of saprotrophic
283 Agaricomycetes⁴⁴.



284

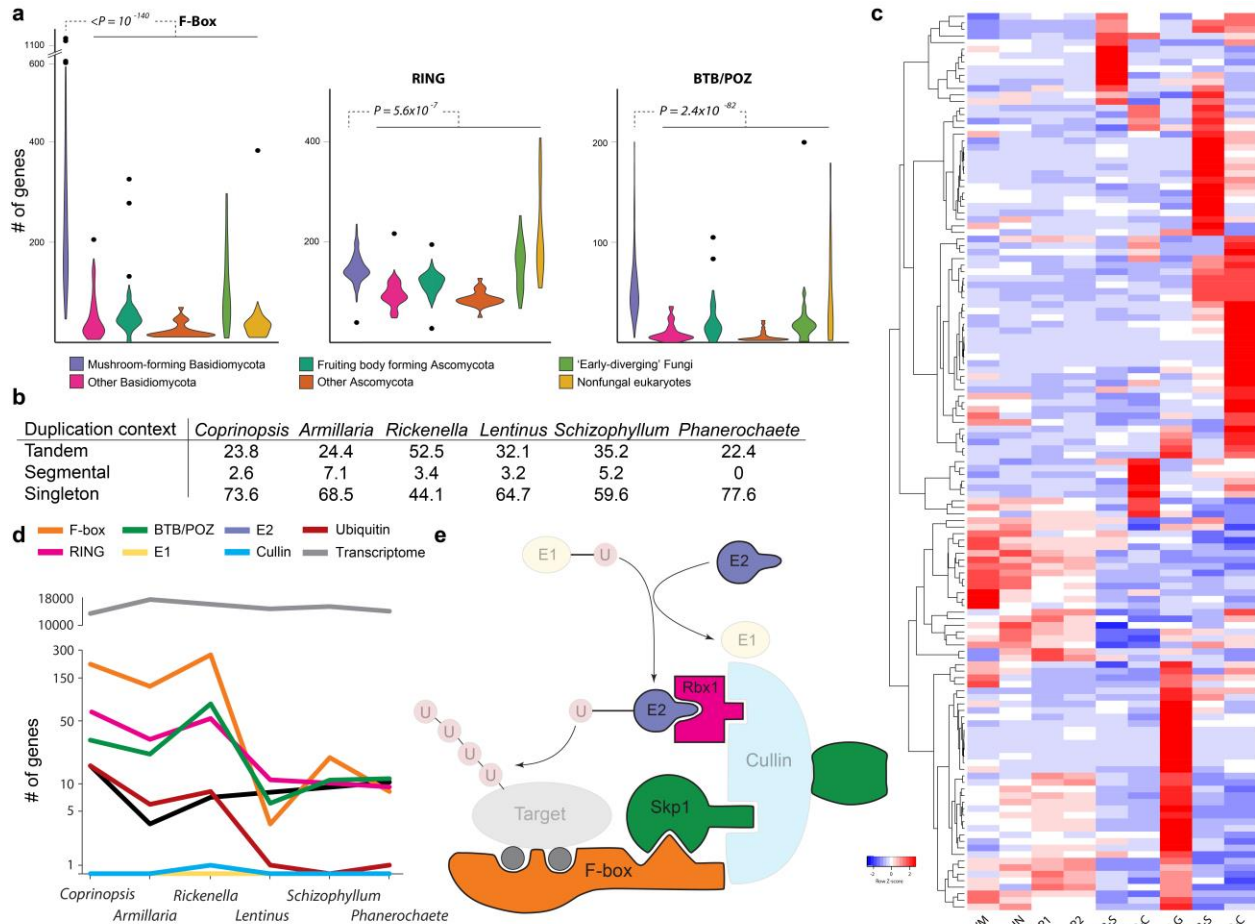
285 **Fig. 3.** Diverse secreted proteins are developmentally regulated in fruiting bodies. **a.** the
 286 distribution of GPI-anchored secreted protein repertoire, its developmentally regulated and
 287 conserved developmentally regulated subsets. **b.** Numbers of all and developmentally regulated
 288 small secreted proteins, with orphan genes shaded differently. **c.** Copy number distribution and
 289 developmental regulation of hydrophobins and cerato-platanins in the six species. **d.** Functional
 290 annotation of small secreted proteins in the six species.

291

292 Targeted protein degradation shows striking expansion in mushrooms

293 We found a strong signal for developmental expression of components the E3 ubiquitin ligase
 294 complex. Several genes encoding F-box proteins, RING-type zinc-finger and BTB/POZ domain
 295 proteins are developmentally regulated in all species, often displaying tissue or developmental
 296 stage-specific expression peaks (Fig. 4, Supplementary Fig. 12). These gene families are also
 297 strongly overrepresented in the genomes of mushroom-forming fungi compared to related
 298 filamentous fungi and yeasts (Fig 4/a). For example, while yeasts and filamentous fungi possess
 299 ~20 and 60-90 F-box proteins⁴⁵, respectively, mushroom-forming fungi have 67-1,199 copies
 300 (mean: 274), comparable to the numbers seen in higher plants⁴⁶ and resulting predominantly
 301 from recent tandem duplications (Fig. 4/b, Supplementary Fig. 13). They mostly showed a single
 302 peak in expression and many of them were upregulated at fruiting body initiation or in caps, gills
 303 and stipes (Fig 4/c). The numbers of developmentally regulated F-box, RING-type zinc-finger
 304 and BTB/POZ domain containing genes found in the six species show a good correlation with
 305 fruiting body complexity but a poor correlation with the number of expressed genes (Fig 4/d),
 306 suggesting a link between the expansion of these genes and the evolution of complex fruiting
 307 body morphologies. These genes define the target specificity of E3 ubiquitin ligases^{45,47}, which
 308 enables a tight regulation of selective proteolysis during development⁴⁶. In plants, F-box
 309 proteins can also act as transcriptional regulators⁴⁸, although this is yet to be proven in fungi. On
 310 the other hand, ubiquitin conjugating (E2) enzymes are developmentally regulated only in
 311 *Coprinopsis*, *Armillaria* and *Rickenella*, whereas ubiquitin activating (E1) enzymes, cullins,

312 SKP1, HECT-type ubiquitin ligases are neither developmentally regulated nor significantly
 313 overrepresented in mushroom-forming fungi (Fig 4/e, $P > 0.05$, FET). With the exception of
 314 *Coprinopsis*, we did not detect specific expression patterns of neddylation and deneddylation
 315 genes as reported for the Ascomycota⁴⁹. Taken together, we observed a striking expansion and
 316 distinctive expression patterns of genes that define target-specificity of the E3 ubiquitin ligase
 317 complex (F-box, RING and BTB/POZ proteins) in Agaricomycetes. This parallels F-box gene
 318 expansion in plants which, combined with their widespread role in development^{46,50}, suggests
 319 that they likely have key roles in complex multicellular development in mushroom-forming fungi.
 320



321
 322 Fig. 4. **a**, Copy number distribution of F-box, RING-type zinc finger and BTB/POZ domain
 323 proteins showing their enrichment in mushroom-forming fungi compared to other fungal groups.
 324 **b**, The context of gene duplications of F-box proteins in the genomes of six analyzed species. **c**,
 325 heatmap of developmentally regulated F-box proteins in *Coprinopsis cinerea*. Genes were
 326 hierarchically clustered based on gene expression similarity using average linkage clustering.
 327 Abbreviations: VM - vegetative mycelium, HN - hyphal knot, P1 - stage 1 primordium, P2 - stage
 328 2 primordium, YFB - young fruiting body, FB - mature fruiting body, '-C' - cap, '-S' - stipe, '-G' -
 329 gills. **d**, The correlation between morphological complexity of fruiting bodies and the number of
 330 developmentally regulated elements of the E3 ligase complex. **e**, Outline of the E3 ubiquitin
 331 ligase complex highlighting members expanded and developmentally regulated (solid) in

332 mushroom-forming fungi. Transparent members are not expanded nor developmentally
333 regulated.

334 Key multicellularity-related genes are developmentally regulated in fruiting 335 bodies

336 Complex multicellularity in fungi is implemented by the reprogramming of hyphal branching
337 patterns, followed by their adhesion and differentiation⁷. This assumes mechanisms for cell-to-
338 cell communication, adhesion, differentiation and defense. We examined the expression
339 dynamics of gene families related to these traits, including transcription factors (TFs), protein
340 kinases, adhesion and defense-related genes. Like other complex multicellular lineages,
341 mushroom-forming fungi make extensive use of transcription factors (TFs) in development. To
342 identify development-related TFs, we manually curated TF candidate genes to exclude ones
343 that nonspecifically bind DNA. The resulting TFomes contain 278-408 genes, of which 4.5-64%
344 were developmentally regulated (Supplementary Fig. 14). These were dominated by C2H2 and
345 Zn(2)C6 fungal type, fungal trans and homeodomain-like TFs (Fig 5/a). Although transcription
346 factor families were usually not conserved, we found 5 TF families that contained
347 developmentally regulated genes from 5 or 6 species (Supplementary Table 10). These
348 included C2H2-type zinc fingers (including *c2h2* of *Schizophyllum*^{14,51}), Zn(2)-C6 fungal-type
349 and homeobox TFs (containing *hom1* of *Schizophyllum*^{14,51}). Two clusters of C2H2 and
350 homeobox TFs showed expression peaks in stipes of *Coprinopsis*, *Lentinus*, *Armillaria* and
351 *Rickenella*, confirming previous reports of *Hom1* expression in *Coprinopsis*⁵² and
352 *Schizophyllum*^{51,53}. Members of the white collar complex were developmentally regulated in all
353 species except *Phanerochaete*, mostly showing a significant increase in expression at initiation.
354 However, these genes did not group into one family in the clustering, which was a common
355 pattern for TF families, perhaps caused by their high rate of sequence evolution.

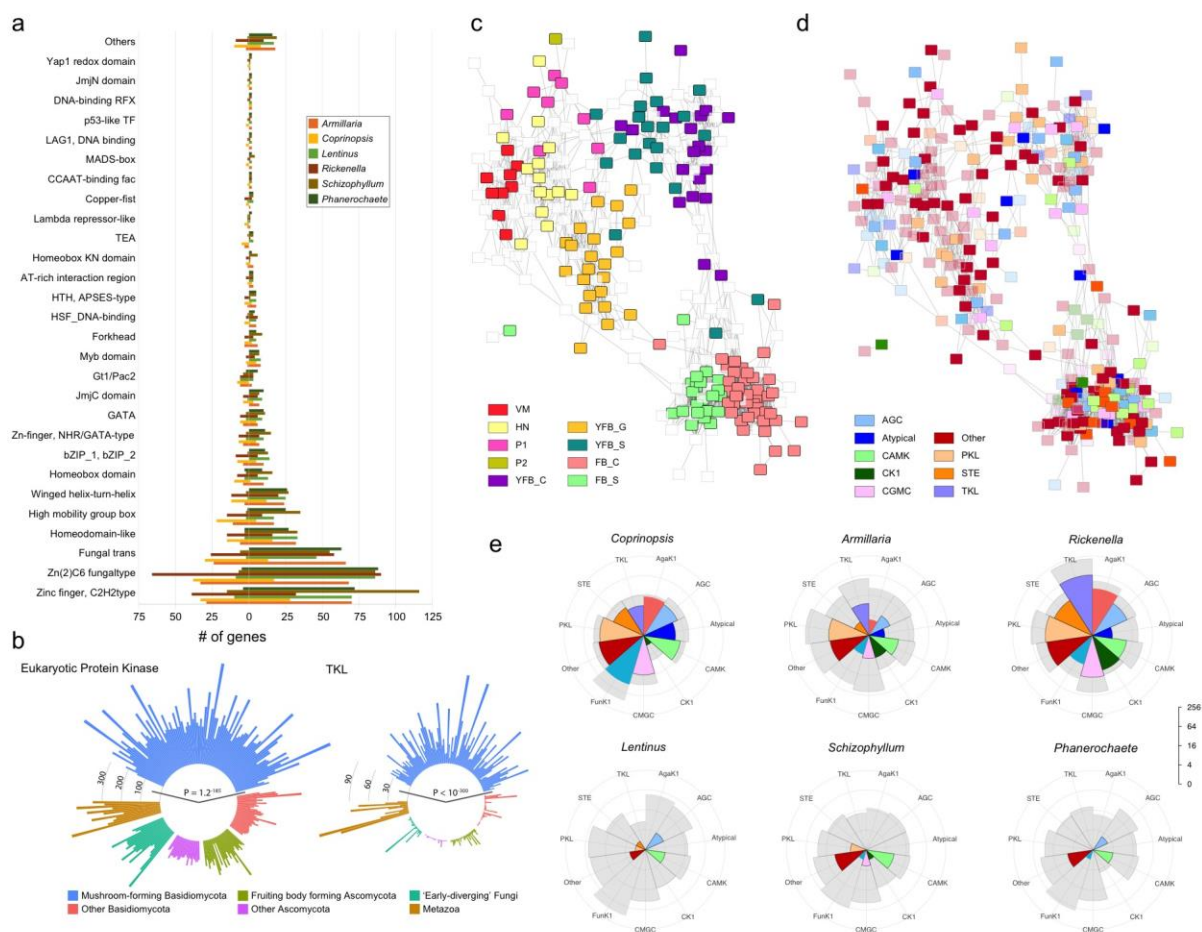
356 Communication among cells by various signaling pathways is paramount to the increase
357 of distinct cell types in evolution. In accordance with the higher complexity of mushroom-forming
358 fungi, their kinomes are significantly larger than that of other fungi ($P = 1.1 \times 10^{-184}$, FET, Fig 5/b),
359 due to expansions of the eukaryotic protein kinase superfamily. We classified protein kinases
360 into nine groups⁵⁴ using published kinome classifications for *Coprinopsis*³. The six mushroom
361 kinomes (Supplementary Table 12) have a similar composition, with PKL, CMGC and CAMK
362 families being most diverse and RGC and tyrosine kinases missing. The Agaricomycetes-
363 specific FunK1 family is expanded significantly, as reported earlier³. Tyrosine kinase-like
364 kinases also show a strong expansion in Agaricomycetes ($P < 10^{-300}$), consistent with
365 observations in *Laccaria bicolor*⁵⁵ and other species⁵⁶. Histidine kinases are underrepresented
366 ($P = 8.95 \times 10^{-36}$) relative to other fungal groups.

367 A kinase co-expression network revealed tissue specificity as the main driver of network
368 topology (Fig 5/c-d), with most kinases showing an expression peak late in development.
369 Kinases with early expression peaks are mostly highly expressed through multiple stages,
370 resembling early expressed modules of *Coprinopsis* (Fig. 1/c, Supplementary Fig. 15). Many
371 CAMK family members showed expression peaks in cap and gill tissues. However, overlaying
372 the network with classification shows no general enrichment of any family in developmental
373 stages or tissues (Fig 5/d-e), indicating diverse co-option events for development at the highest

374 level of kinase classification. The FunK1 family has been linked to multicellular development,
375 based on an upregulation in fruiting bodies³. In our species FunK1 comprises 4-33% of the
376 kinome and 0.2-35% of the developmentally regulated kinases, although this Fig. resembles
377 that of other kinase families. Members of the highly expanded tyrosine kinase like (TKL) family
378 (Fig 5/e) are developmentally regulated in *Coprinopsis*, *Armillaria* and *Rickenella*, but not in
379 species with simpler morphologies. The expansion and developmental expression of the TKL
380 family in mushroom-forming fungi is a remarkable case of convergence with complex
381 multicellular plants^{57,58} and animals⁵⁸ and may be related to parallel increases in organismal
382 complexity. Yet, while most plant TKL genes have receptor-like architectures⁵⁹, we found no
383 evidence of extracellular domains or secretion signals in TKL genes of mushroom-forming fungi,
384 suggesting they orchestrate signal transduction via soluble kinases or other mechanisms
385 different from those of multicellular plants and animals.

386 Fungal immune systems comprise innate chemical defense mechanisms against
387 metazoan predators and bacterial and fungal infections⁶⁰. We catalogued eleven families of
388 defense effector proteins and their expression to assess the conservation of the defensive
389 arsenal of Agaricomycetes. Genomes of mushroom-forming fungi harbor highly species-specific
390 combinations of defense-related genes encoding pore-forming toxins, cerato-platanins, lectins
391 and copsins, among others, with most of them being developmentally expressed and
392 upregulated at fruiting body initiation (Supplementary Fig 16). Of the eleven families only three
393 were conserved, and only one (thaumatins) was developmentally regulated in all six species,
394 which can display either endoglucanase or antimicrobial activity, depending on the structure of
395 the mature protein. *In silico* structure prediction identified an acidic cleft in fruiting body
396 expressed thaumatins (Supplementary Fig 16), consistent with an antimicrobial activity. Several
397 defense-related lectins have been reported from fruiting bodies⁶¹, although lectins have been
398 implicated in cell adhesion and signaling too. Agaricomycete genomes encode at least 17 lectin
399 and 2 lectin-like families, of which seven are significantly overrepresented ($P < 0.05$, FET,
400 Supplementary Table 3). Developmentally regulated lectins belong to nine families, with 4-7
401 family per species, but only ricin B lectins were developmentally regulated in all six species
402 (Supplementary Fig 17). Other lectin families show a patchy phylogenetic distribution, which is
403 also reflected in their expression patterns in fruiting bodies. Several lectins are induced at
404 fruiting body initiation, including all previously reported nematotoxic *Coprinopsis* lectins (CCL1-
405 2, CGL1-3 and CGL3). Taken together, the defense effector and lectin-encoding arsenal of
406 mushroom-forming fungi shows a patchy phylogenetic distribution, consistent with high gene
407 turnover rates or gains via horizontal gene transfer⁶⁰. Accordingly, expressed defense gene sets
408 are highly species-specific, with most of the encoded genes upregulated in fruiting bodies,
409 suggesting that chemical defense is a key fruiting body function.

410
411



412
413 **Fig. 5.** Expression and copy number distribution of transcription factor and kinase genes. **a.**
414 transcription factor family distribution and the proportions of developmentally regulated (left)
415 versus not regulated (right) genes across six species. **b.** Circular bar diagram of eukaryotic
416 protein kinase (left) and tyrosine kinase-like (right) repertoires of mushroom-forming fungi
417 versus in other fungal groups and non-fungal eukaryotes. P values of overrepresentation in
418 mushroom-forming fungi are given for both plots. **c** and **d.** Co-expression network of 306
419 expressed kinases of *Coprinopsis cinerea* overlaid with expression peak (**c**) and kinase
420 classification (**d**). Pairwise correlation coefficients of expression profile similarity were calculated
421 for each pair of kinase genes and networks were visualized with a correlation coefficient cutoff
422 of 0.825. **e.** Kinome (grey fill) and developmentally regulated kinome (solid fill) repertoires of the
423 six species split by kinase classification. The families Funk1 and Agak1 of the 'Other' group are
424 shown separately. Axes are transformed to \log_2 scale.

425 Discussion

426 We charted the transcriptomic landscape of multicellular development in 6 phylogenetically
427 diverse mushroom-forming species and performed comparative analyses of >200 genomes. We
428 pinpointed nearly 300 conserved gene families, and another 73 gene groups with
429 developmentally dynamic expression in ≥ 5 species, as well as 631 domains significantly
430 overrepresented in mushroom-forming fungi. These are enriched in cell wall modifying

431 enzymes, various secreted proteins (including GPI-anchored and small secreted proteins),
432 components of the ubiquitin ligase complex, kinases or transcription factors. Lectins and
433 defense effectors, on the other hand, showed species-specific repertoires, indicating a higher
434 rate of evolutionary turnover. These data provide a framework for elucidating the core genetic
435 program of fruiting body formation and will serve as guideposts for a systems approach to
436 understanding the genetic bases of mushroom development and multicellularity.

437 Complex multicellularity evolved in five lineages, of which plants, animals and fungi are
438 the most diverse^{7,58}. At the broadest level of comparison, these lineages evolved similar
439 solutions to cell adhesion, communication, long-range transport and differentiation^{58,62,63}. As in
440 animals and plants, protein kinases, putative adhesive proteins, defense effectors, and certain
441 transcription factors have expanded repertoires in mushroom-forming fungi and show
442 developmentally dynamic expression patterns. Examples for convergent expansions in
443 mushroom-forming fungi, in plants and/or animals include TKL family kinases, F-box proteins
444 and cadherins, indicating that ancient eukaryotic gene families with apt biochemical properties
445 have been repeatedly co-opted for complex multicellularity during evolution. F-box proteins
446 showed the largest expansion in Agaricomycetes across all families and was the largest
447 developmentally regulated family, along with RING-type and BTB domain proteins. Among
448 independently evolved fruiting body forming fungi^{7,49,64}, Agaricomycetes share some similarity
449 with the Pezizomycotina (Ascomycota), many of which also produce macroscopic fruiting
450 bodies. For example, laccases, lectins, several transcription factors and signal transduction
451 systems have also been implicated in fruiting body formation in the Pezizomycotina, although at
452 the moment it is unclear how frequently convergent expansions and co-option events can be
453 observed in independently evolved lineages of complex multicellular fungi⁷.

454 Mushroom-forming fungi also show several unique solutions for multicellularity, as
455 expected based on their independent evolutionary origin. These are, in part, explained by the
456 very nature of fungi: complex multicellularity comprises the reproductive phase of the life cycle
457 (except in sclerotia, rhizomorphs) and so mechanisms have evolved for sensing when fruiting
458 body formation is optimal (e.g. nutrient availability, light). Mushroom development can be
459 partitioned into an early phase of cell proliferation and differentiation and a growth phase of
460 rapid cell expansion, a division evident on gene co-expression profiles as well. Broadly
461 speaking, this is similar to the development of fleshy plant fruits, although mechanisms are likely
462 to be convergent, like many other aspects of mushroom development.

463 This work has provided a glimpse into the core genetic toolkit of complex multicellularity
464 in mushroom-forming fungi. Our comparative transcriptomic genomic analyses revealed gene
465 families, most of which reported as novel, with conserved developmental expression in fruiting
466 bodies, with scope to increase the resolution both phylogenetically and among cell types (e.g.
467 by single-cell RNA-Seq). Such data should help defining the conserved genetic programs
468 underlying multicellularity in mushroom-forming fungi, and uncovering the evolutionary origins of
469 a major complex multicellular lineage in the eukaryotes.

470

471 Methods

472 Strains, fruiting protocols and nucleic acid extraction

473 For fruiting *Coprinopsis cinerea* strain #326 (*A43mut B43mut pab 1-1*) an agar disk (5 mm in
474 diameter) was placed on the center of YMG/T agar media (4 g yeast extract, 10 g malt extract, 4
475 g glucose, 10 g agar media with 100 mg tryptophane added after cooling⁶⁵) at 37 °C for five
476 days in the dark. When the colonies reached the 1-2 mm distance from the edge of Petri dishes
477 they were placed into 25 °C for one week in a 12 hrs light/12 hrs dark cycle for fruiting. Fruiting
478 body stages were defined following standard conventions⁵. Exact alignment of developmental
479 stages across species was impossible, but we made an attempt to define functionally putatively
480 homogeneous stages to follow the general notation of mushroom developmental stages as
481 closely as possible in each species. Nevertheless, the array of sample types differed from
482 species to species, due to the morphological diversity of fruiting bodies or limitations in
483 dissectability. In *Coprinopsis*, vegetative mycelium, hyphal knot, stage 1 and stage 2 primordia,
484 young fruiting body cap, gills and stipe, fruiting body cap and stipe were harvested for RNA
485 extraction. The hyphal knot stage was defined as an up to 0.5 mm diameter condensed hyphal
486 aggregate. Stage 1 primordia were defined as up to 2 mm tall shaft like structures, while stage 2
487 primordia up to 4 mm tall fruiting body initials with visible differentiation of cap and stipe initials.
488 Young fruiting bodies were up to 15 mm tall with a slightly elongated stipe and immature
489 basidia. Fruiting bodies had fully extended stipes and caps, being in an early autolytic phase.

490 Before fruiting, *Schizophyllum commune* the H4-8a and H4-8b monokaryons⁴ were
491 grown on MM medium according to Dons et. al.⁶⁶. After dikaryon formation an agar plug (5 mm)
492 was placed on the center of fresh MM medium at 30 °C for five days in the dark, then it was
493 placed at 25 °C for 10 days in a 12/12 hrs light/dark cycle (cool white F18w/840), upside down.
494 Dikaryotic vegetative mycelium, stage 1 and 2 primordia, young fruiting body and fruiting body
495 stages were harvested for RNA-seq. We defined stage 1 primordia as up to 2 mm fruiting body
496 initials, stage 2 primordia as 3-4 mm tall initials with an apical pit on the top, the young fruiting
497 body as a 5-7 mm tall cup-like structure with visible pseudolamellae inside, while fully expanded
498 ones were considered fruiting body.

499 Vegetative mycelia of *Lentinus tigrinus* RLP-9953-sp were maintained on MEA (20 g
500 malt extract, 0.5 g yeast extract, 15 g agar for 1L). For fruiting a mycelial plug was placed (5 mm
501 diameter) on modified sawdust-rice bran medium⁶⁷ (1 part wheat bran and 2 parts aspen
502 sawdust wetted to 65% moisture for 100 ml in a 250 ml beaker). The culture was incubated for
503 21 days at 30 °C in the dark, then placed in a moist growth chamber at 25 °C in a 12/12 hour
504 light/dark cycle. Vegetative mycelia, stage 1 primordia, stage 2 primordia cap and stipe, young
505 fruiting body cap and stipe and fruiting body cap and stipe tissues were harvested for RNA-Seq.
506 Stage 1 primordium was defined as a 5-20 mm tall white stalk-structure without any
507 differentiation of a cap initial, stage 2 primordium was defined as a 15 – 25 mm tall stalk-like
508 structure with a brown apical pigmentation (cap initial), young fruiting body had and up to 5 mm
509 wide brown cap initial with just barely visible gills on the bottom, growing on a 30-40 mm tall
510 stipe, fruiting body was 50-70 mm tall, with fully flattened (but not funnel-shaped) cap.

511 *Phanerochaete chrysosporium* RP-78 was fruited on YMPG media (10 g glucose, 10 g
512 malt extract, 2 g peptone, 2 g yeast extract, 1 g asparagine, 2 g KH₂PO₄, 1 g MgSO₄ x 7 H₂O,
513 20 g agar for 1L with 1 mg thiamine added after cooling) covered with cellophane for 7 days at
514 37 °C in the dark, then placed in a moist growth chamber at 25 °C in an area with dimmed
515 ambient light conditions, following the recommendations of Jill Gaskell (US Forest Products
516 Laboratory, Washington, D. C., USA). Vegetative mycelium, young fruiting body and fruiting

517 body stages were harvested for RNA extraction. Young fruiting body stage was defined as
518 fruiting body initials that forms a compact mat well-delimited from the surrounding vegetative
519 mycelium, while the fruiting bodies were harvested just after they started releasing spores
520 (visible on the lids of Petri dishes).

521 *Rickenella mellea* SZMC22713 was cultured on Fries Agar⁶⁸ for harvesting vegetative
522 mycelium for RNA and DNA extraction. DNA for genome sequencing was extracted using the
523 Blood & Cell Culture DNA Maxi Kit (Qiagen) from 300 mg finely ground mycelium powder
524 according to the manufacturer's instructions. The internal transcribed spacer region was PCR
525 amplified and sequenced to verify strain identity. For RNA-Seq, fruiting body stages were
526 collected in November 2016 from Kistelek, Hungary (approx. coordinates: 46.546309,
527 19.954507). Stage 1 primordium was defined as an approximately 1 mm tall, shaft-like, pear-
528 shaped structure, without any visible cap initial, stage 2 primordium was described as a 2-3 mm
529 tall structure with a small cap initial, young fruiting body was defined by the 5-15 mm tall
530 structure with a 1-2 mm wide cap, and the fruiting body was characterized by a fully expanded
531 cap on the top of a 20-32 mm tall stipe.

532 Data for *Armillaria ostoyae* C18/19 were taken from our previous study¹⁶, with the
533 following stages defined: vegetative mycelium, stage 1 primordium, stage 2 primordium cap and
534 stipe, young fruiting body cap and stipe, and fruiting body cap, stipe and gills.

535 For RNA extraction all samples were immediately placed on liquid nitrogen after
536 harvesting and stored at -80 °C until use. Frozen tissues were weighed and 10-20 mg of *C.*
537 *cinerea*, *S. commune*, *P. chrysosporium* and *R. mellea* and 50-75 mg of *L. tigrinus* were
538 transferred to a pre-chilled mortar and ground to a fine powder using liquid nitrogen. We
539 extracted RNA of *C. cinerea*, *S. commune*, *P. chrysosporium* and *R. mellea* using the Quick-
540 RNA™ Miniprep (Zymo Research), or the RNeasy Midi Kit (QIAGEN) for *L. tigrinus*. Both of the
541 kits were used according to the manufacturer's instructions.

542

543 **De novo draft genome for *Rickenella mellea***

544 The genome and transcriptome of *Rickenella mellea* were sequenced using Illumina platform.
545 The genomes were sequenced as pairs of Illumina standard and Nextera long mate-pair (LMP)
546 libraries. For the Illumina Regular Fragment library, 100 ng of DNA was sheared to 300 bp using
547 the Covaris LE220 and size selected using SPRI beads (Beckman Coulter). The fragments
548 were treated with end-repair, A-tailing, and ligation of Illumina compatible adapters (IDT, Inc)
549 using the KAPA-Illumina library creation kit (KAPA biosystems).

550 For the Illumina Regular Long-mate Pair library (LMP), 5 ug of DNA was sheared using
551 the Covaris g-TUBE(TM) and gel size selected for 4 kb. The sheared DNA was treated with end
552 repair and ligated with biotinylated adapters containing *loxP*. The adapter ligated DNA
553 fragments were circularized via recombination by a Cre excision reaction (NEB). The
554 circularized DNA templates were then randomly sheared using the Covaris LE220 (Covaris).
555 The sheared fragments were treated with end repair and A-tailing using the KAPA-Illumina
556 library creation kit (KAPA biosystems) followed by immobilization of mate pair fragments on
557 streptavidin beads (Invitrogen). Illumina compatible adapters (IDT, Inc) were ligated to the mate
558 pair fragments and 8 cycles of PCR was used to enrich for the final library (KAPA Biosystems).

559 Stranded cDNA libraries were generated using the Illumina Truseq Stranded RNA LT kit.
560 mRNA was purified from 1 µg of total RNA using magnetic beads containing poly-T oligos.

561 mRNA was fragmented and reversed transcribed using random hexamers and SSII (Invitrogen)
562 followed by second strand synthesis. The fragmented cDNA was treated with end-pair, A-tailing,
563 adapter ligation, and 8 cycles of PCR.

564 The prepared libraries were quantified using KAPA Biosystem's next-generation
565 sequencing library qPCR kit and run on a Roche LightCycler 480 real-time PCR instrument. The
566 quantified libraries were then multiplexed with other libraries, and the pool of libraries was then
567 prepared for sequencing on the Illumina HiSeq sequencing platform utilizing a TruSeq paired-
568 end cluster kit, v4, and Illumina's cBot instrument to generate a clustered flow cell for
569 sequencing. Sequencing of the flow cell was performed on the Illumina HiSeq2500 sequencer
570 using HiSeq TruSeq SBS sequencing kits, v4, following a 2x150 indexed run recipe (2x100bp
571 for LMP).

572 Genomic reads from both libraries were QC filtered for artifact/process contamination
573 and assembled together with AllPathsLG v. R49403⁶⁹. Illumina reads of stranded RNA-seq data
574 were used as input for de novo assembly of RNA contigs, assembled into consensus
575 sequences using Rnnotator (v. 3.4)⁷⁰. Both genomes were annotated using the JGI Annotation
576 Pipeline and made available via the JGI fungal portal MycoCosm⁷¹. Genome assemblies and
577 annotation were also deposited at DDBJ/EMBL/GenBank under the accession XXXXX (TO BE
578 PROVIDED UPON PUBLICATION).

579

580 **RNA-Seq**

581 Whole transcriptome sequencing was performed using the TrueSeq RNA Library Preparation Kit
582 v2 (Illumina) according to the manufacturer's instructions. Briefly, RNA quality and quantity
583 measurements were performed using RNA ScreenTape and Reagents on TapeStation (all from
584 Agilent) and Qubit (ThermoFisher); only high quality (RIN >8.0) total RNA samples were
585 processed. Next, RNA was DNaseI (ThermoFisher) treated and the mRNA was purified and
586 fragmented. First strand cDNA synthesis was performed using SuperScript II (ThermoFisher)
587 followed by second strand cDNA synthesis, end repair, 3'-end adenylation, adapter ligation and
588 PCR amplification. All of the purification steps were performed using AmPureXP Beads
589 (Backman Coulter). Final libraries were quality checked using D1000 ScreenTape and
590 Reagents on TapeStation (all from Agilent). Concentration of each library was determined using
591 either the QPCR Quantification Kit for Illumina (Agilent) or the KAPA Library Quantification Kit
592 for Illumina (KAPA Biosystems). Sequencing was performed on Illumina instruments using the
593 HiSeq SBS Kit v4 250 cycles kit (Illumina) or the NextSeq 500/550 High Output Kit v2 300
594 cycles (Illumina) generating >20 million clusters for each sample.

595

596 **Bioinformatic analyses of RNA-Seq data**

597 RNA-Seq analyses were carried out as reported earlier¹⁶. Paired-end Illumina (HiSeq, NextSeq)
598 reads were quality trimmed using the CLC Genomics Workbench tool version 9.5.2 (CLC
599 Bio/Qiagen) removing ambiguous nucleotides as well as any low quality read end parts. Quality
600 cutoff value (error probability) was set to 0.05, corresponding to a Phred score of 13. Trimmed
601 reads containing at least 40 bases were mapped using the RNA-Seq Analysis 2.1 package in
602 CLC requiring at least 80% sequence identity over at least 80% of the read lengths; strand
603 specificity was omitted. List of reference sequences is provided as Supplementary table 1.
604 Reads with less than 30 equally scoring mapping positions were mapped to all possible

605 locations while reads with more than 30 potential mapping positions were considered as
606 uninformative repeat reads and were removed from the analysis.

607 “Total gene read” RNA-Seq count data was imported from CLC into R version 3.0.2.
608 Genes were filtered based on their expression levels keeping only those features that were
609 detected by at least five mapped reads in at least 25% of the samples included in the study.
610 Subsequently, “calcNormFactors” from “edgeR” version 3.4.2⁷² was used to perform data
611 scaling based on the “trimmed mean of M-values” (TMM) method⁷³. Log transformation was
612 carried out by the “voom” function of the “limma” package version 3.18.13⁷⁴. Linear modeling,
613 empirical Bayes moderation as well as the calculation of differentially expressed genes were
614 carried out using “limma”. Genes showing at least four-fold gene expression change with an
615 FDR value below 0.05 were considered as significant. Multi-dimensional scaling (“plotMDS”
616 function in edgeR) was applied to visually summarize gene expression profiles revealing
617 similarities between samples. In addition, unsupervised cluster analysis with Euclidean distance
618 calculation and complete-linkage clustering was carried out on the normalized data using
619 “heatmap.2” function from R package “gplots”.

620

621 **Identification of developmentally regulated genes**

622 We considered genes with a Fragments Per Kilobase Million (FPKM) value >1 to have a non-
623 zero expression. Because differentially expressed genes can only be defined in pairwise
624 comparisons of samples and thus didn’t suit our developmental series data, we opted to use the
625 concept of developmentally regulated gene. These were defined as any gene showing an over
626 four-fold change in expression between any two developmental stages or tissue types and a
627 maximum expression level of FPKM > 4 in at least one developmental stage. Comparisons
628 between tissue types were only performed within the respective developmental stage. We
629 distinguished developmentally regulated genes that showed over four-fold upregulation at
630 fruiting body initiation (‘FB-init’ genes) and those that show over four-fold expression dynamics
631 (up- or downregulation) across the range of fruiting body stages (‘FB genes’, i.e. vegetative
632 mycelium excluded). Note that this strategy excludes genes showing highest expression in
633 vegetative mycelium and no dynamics later on, to remove genes with a significant
634 downregulation at the onset of fruiting body development (e.g. those involved in nutrient
635 acquisition by the mycelium).

636

637 **Comparative genomic approaches**

638 To obtain characteristic Interpro domain signatures of Agaricomycetes, we assembled a dataset
639 comprising genomes of 201 species; ranging from simple unicellular yeasts to filamentous and
640 complex multicellular fungi. InterProScan version 5.24-63.0 was used to perform IPR searches.
641 The 201 species were categorized into two major groups; mushroom-forming fungi (113
642 species) and all other fungi (88 species, 1 Cryptomycota, 2 Microsporidia, 2
643 Neocallimastigomycota, 3 Chytridiomycota, 2 Blastocladiomycota, 14 Zygomycota, 1
644 Glomeromycota, 38 Ascomycota, 20 non-fruiting body forming Basidiomycota). The enrichment
645 of IPR domains was tested using Fisher’s exact test and corrected for multiple testing by the
646 Benjamini-Hochberg method in R (R core team 2016). $P < 0.01$ was considered significant.
647 Significantly overrepresented IPR domains were characterized by Gene Ontology Terms using
648 IPR2GO.

649 An all-versus-all protein BLAST was performed for the six species (*A. ostoyae*, *C.*
650 *cinerea*, *S. commune*, *L. tigrinus*, *P. chrysosporium*, *R. mellea*) and for the 201-species dataset
651 using mpiBLAST (v.1.6.0) with default parameters. Clustering was done using Markov Cluster
652 with an inflation parameter of 2.0²⁵.

653

654 **Reconstruction of alternative splicing patterns**

655 We reconstructed patterns of alternative splicing using the RNA-Seq data for all six species. To
656 this end, we used region-restricted probabilistic modelling (RRPM)²¹ to discover alternative
657 transcripts, as described by Gehrman et al.. Briefly, the genome was split at gene boundaries
658 into fragments, then all RNA-Seq reads were aligned to these fragments with STAR v2.5.3a⁷⁵, in
659 two rounds. The first round of read alignment was run to produce a novel splice junction
660 database, which was used to improve mapping in the second round. Using the BAM file from
661 this alignment, Cufflinks v2.2.1⁷⁶ was run in RABT mode to predict novel transcripts. To restore
662 the context, these sets of transcripts were projected back onto the original annotation. The
663 resulting annotation file was filtered to remove predicted transcripts with no detectable
664 expression (FPKM = 0) or did not have reads supporting its splice junctions. We performed read
665 alignment using STAR again with the same two round method and the new, corrected
666 annotation file and used the Cufflinks suite to estimate the expression level for each transcript.
667 We then aligned reads of each RNA-Seq replicate separately to the genome with updated gene
668 annotation. This resulted in an expression profile for each alternatively spliced transcript, in
669 every developmental stage. We subsequently identified developmentally regulated transcripts
670 using the same functions as described above for genes. For splicing event discovery, we used
671 the ASpli⁷⁷ R package where we used the most significant transcript (the most abundant
672 transcript through the developmental stages) as the reference for event discovery. Custom
673 scripts were used to extract stage and tissue-type specificity and distribution of spliced genes
674 and splicing events.

675

676 **Phylostratigraphic analysis**

677 To examine the evolutionary origin of developmentally regulated genes in each species, a
678 phylostratigraphic analysis was performed¹⁹. First, we assembled a database containing
679 genomes covering the evolutionary route from the most recent common ancestor of cellular
680 organisms to the respective species, by complementing the database of Drost et al.²⁰. Fungal,
681 microsporidia and plant genomes were removed from this database and substituted by 416
682 fungal genomes (all published), including 382 belonging to the Dikarya and 116 to the
683 Agaricomycetes. In addition, 6 microsporidia, 59 plant and 6 Opisthokonta⁷⁸ genomes were
684 added, resulting in a database of 4,483 genomes. The database was divided into age
685 categories ('phylostrata') based on the tree available at Mycocosm⁷¹ and the eukaryotic tree
686 published by Torruella et al.⁷⁸. The oldest phylostratum consisted of bacteria and archaea.
687 Whole proteomes of *Coprinopsis cinerea*, *Armillaria ostoyae*, *Schizophyllum commune*,
688 *Lentinus tigrinus*, *Phanerochaete chrysosporium* and *Rickenella mellea* were blasted against
689 this database using mpiblast 1.6.0⁷⁹ with default settings. Blast hits were filtered with an E-value
690 cut-off of 1×10^{-6} and a query coverage cut-off of 80%. After filtering, the age of each gene was

691 defined as the node of the tree representing the last common ancestor of the species sharing
692 homologs of the gene, at the specified blast cutoff.

693 To infer what Agaricomycete-specific genes are preferentially developmentally
694 regulated, we analyzed the enrichment of annotation terms among developmentally regulated
695 genes specific to Agaricomycetes compared to developmentally regulated genes whose origin
696 predates the Agaricomycetes. To this end, we divided the phylostratigraphy profiles into two
697 groups, corresponding to genes that originated before and those that originated after the origin
698 of mushroom-forming fungi (Phylostratum 18). We tested for significant enrichment of IPR
699 domains (evaluate $< 1e-5$) in developmentally regulated genes that originated within the
700 Agaricomycetes, relative to the other group of more ancient developmentally regulated genes
701 using Fisher's exact test ($P < 0.05$).

702

703 **CAZyme annotation**

704 Genes encoding putative carbohydrate-active enzymes were annotated using the CAZy
705 pipeline. BLAST and Hmmer searches were conducted against sequence libraries and HMM
706 profiles in the CAZy database⁸⁰ (<http://www.cazy.org>). Positive hits were validated manually and
707 assigned a family and subfamily classification across Glycoside Hydrolase (GH), Carbohydrate
708 Esterase (CE), Glycoside Transferase (GT), Polysaccharide Lyase (PL), Carbohydrate-Binding
709 Module (CBM) and Auxiliary redox enzyme (AA) classes of the CAZy system⁸¹. Activities were
710 determined by BLAST searches against biochemically characterized subsets of the CAZy
711 database.

712

713 **Coexpression analysis**

714 Developmentally regulated genes in each species were clustered into co-expression modules
715 based on their expression dynamics by using the clustering method implemented in Short Time-
716 series Expression Miner (STEM v. 1.3.11)^{18,82}. Default parameters were used, except minimum
717 absolute expression change, which was set to 4. Functional annotations of modules were
718 obtained by GO enrichment analyses in TopGO (see below). For a higher-level grouping of co-
719 expression modules, we defined six categories corresponding to early and late expressed
720 genes, cap, stipe and gill specific genes and a mixed category. Coexpression modules were
721 placed in one of these categories if more than half of the module's members had the same
722 tissue- or stage-specific expression peaks. Modules without stage or tissue specificity were
723 grouped in the mixed category. The early expressed category included coexpression modules
724 with expression peaks in H, P1 or P2 stages, while late module category consisted of modules
725 with young fruiting body and fruiting body stage specific expression peaks. We functionally
726 annotated the modules and higher categories using InterPro Scan v5.24-63.0.

727 To visualize the kinase expression network across various kinase groups and
728 developmental stages, a co-expression network was visualized using Cytoscape v3.6.1 based
729 on pairwise Pearson correlation coefficients for kinase expression patterns in *Coprinopsis*
730 *cinerea*. Pairwise Pearson correlations coefficients for each kinase gene pair were calculated
731 and a 0.85 cut-off was applied for network construction.

732

733 **Functional annotations, GO and Interpro enrichment**

734 Gene Ontology (GO) enrichment analyses were carried out for developmentally regulated
735 genes. For this, we annotated genes with GO terms based on their InterPro domain contents.
736 Analyses were performed using Fisher's exact test with threshold $P < 0.05$ in the R package
737 topGO. The parameter algorithm weighted01 was chosen. Heatmaps were created using the
738 heatmap.2 function of the R package 'gplots'. Unsupervised cluster analysis with Pearson's
739 distance calculation and averaged-linkage clustering was carried out on the FPKM values, and
740 heatmaps was visualised using z-score normalization on the rows via the heatmap.2 function.

741 Prediction of glycosylphosphatidylinositol anchored proteins (GPI-Ap) for the six species
742 was performed using the portable version of Pred-GPI⁸³. From the proteins with a predicted
743 GPI-anchor, we excluded ones which had no extracellular signal sequence, as assessed by
744 SignalP version 4.1⁸⁴. Prediction of Small Secreted Proteins (SSP) for the six species was
745 performed using a modified version of the bioinformatic pipeline of Pellegrin et al.⁴⁴. Proteins
746 shorter than 300 amino acids were subjected to signal peptide prediction in SignalP (version
747 4.1) with the option "eukaryotic". Extracellular localisation of these proteins was checked with
748 WoLFPSort version 0.2⁸⁵ using the option "fungi". Proteins containing transmembrane helix not
749 overlapping with the signal peptide were also excluded. Prediction of transmembrane helices
750 was performed with TMHMM (version 2.0)⁸⁶. Finally, proteins containing a KDEL motif (Lys-Asp-
751 Glu-Leu) in the C-terminal region (prosite accession "PS00014") responsible for retention in the
752 endoplasmic reticulum (ER) lumen, were identified using PS-SCAN ([http://www.hpa-
753 bioinfotools.org.uk/cgi-bin/ps_scan/ps_scanCGI.pl](http://www.hpa-bioinfotools.org.uk/cgi-bin/ps_scan/ps_scanCGI.pl)) and excluded.

754 We identified transcription factors based on the presence of InterPro domains with
755 sequence-specific DNA-binding activity retrieved from literature data^{87,88} and manual curation of
756 the Interpro-database. Annotated genes were then filtered based on their domain architecture in
757 order to discard genes encoding DNA-binding proteins with functions other than transcription
758 regulation (such as DNA-repair, DNA-replication, translation, meiosis).

759 We extracted the putative kinase genes from the 6 species based on their InterPro
760 domain composition, and manually curated the classical kinases by excluding domains which
761 correspond to metabolism related kinases and other non-classical protein kinases. The set of
762 proteins having kinase related domains (Supplementary table 12) were subjected to BLAST
763 searches (*BLAST 2.7.1+*, E-value 0.001) against the kinome of *Coprinopsis cinerea*³
764 downloaded from Kinbase (www.kinase.com). The best hits for the six species were classified
765 into eukaryotic protein kinase (ePK) and atypical protein kinases (aPK) and their families and
766 subfamilies as described in the hierarchical kinase classification system⁵⁴.

767 Acknowledgements

768 The authors thank Daniel Cullen and Jill Gaskell (USDA, USA) for the strain of *Phanerochaete*
769 used in this study. This work was supported of the Momentum Program of the Hungarian
770 Academy of Sciences (Contract No: LP2014/12), and of the National Research, Development
771 and Innovation Office (Grant No: GINOP-2.3.2-15-2016-00001). This project has received
772 funding from the European Research Council (ERC) under the European Union's Horizon 2020
773 research and innovation programme (grant agreement number 758161 and 716132). The work
774 by the U.S. Department of Energy Joint Genome Institute, a DOE Office of Science User
775 Facility, is supported by the Office of Science of the U.S. Department of Energy under Contract
776 No. DE-AC02-05CH11231.

777 Author contributions

778 K.K. and L.G.N. conceived the study. K.K., B.K., E.A. performed fruiting experiments, RNA
779 isolation and data analysis. B.B., I.N., J.C. obtained and analysed RNA-Seq data. Z.M., N.S.,
780 M.V., T.K. and L.G.N. performed comparative genomic and phylogenomic analyses. S.M.
781 analyzed the genomic context of F-box gene duplications. B.H. analyzed CAZymes. E.A. and
782 R.A.O. analyzed transcription factors. B.H. contributed valuable analytical insights. K.B., J.J.,
783 A.L., J.P., J.Y. Y.X. and I.V.G. sequences, assembled and annotated the genome of *Rickenella*
784 *mellea*. L.G.N., K.K., B.B., and U.K. wrote the manuscript. D.S.H. contributed the genome of
785 *Lentinus tigrinus* and analytical insights. All authors read and commented on the manuscript.

786 Data availability

787 Genome assembly and annotation of *Rickenella mellea* was deposited at DDBJ/
788 EMBL/GenBank under the accession XXXXXX (to be provided upon publication). A Gene
789 Expression Omnibus (GEO) archive of the sequenced *A. ostoyae* libraries was deposited in the
790 NCBI's GEO Archive at <http://www.ncbi.nlm.nih.gov/geo> under accession SRP109671.

791 References

- 792 1. Kohler, A. *et al.* Convergent losses of decay mechanisms and rapid turnover of
793 symbiosys genes in mycorrhizal mutualists. *Nat. Genet.* **47**, 410-415, (2015).
- 794 2. Kalaras, M. D., Richie, J. P., Calcagnotto, A. & Beelman, R. B. Mushrooms: A rich source
795 of the antioxidants ergothioneine and glutathione. *Food Chem.* **233**, 429–433 (2017).
- 796 3. Stajich, J. E. *et al.* Insights into evolution of multicellular fungi from the assembled
797 chromosomes of the mushroom *Coprinopsis cinerea* (*Coprinus cinereus*). *Proc Natl Acad*
798 *Sci U S A* **107**, 11889–11894 (2010).
- 799 4. Ohm, R. A. *et al.* Genome sequence of the model mushroom *Schizophyllum commune*.
800 *Nat. Biotechnol.* **28**, 957–963 (2010).
- 801 5. Kues, U. Life history and developmental processes in the basidiomycete *Coprinus*
802 *cinereus*. *Microbiol Mol Biol Rev* **64**, 316–353 (2000).
- 803 6. Kues, U. & Navarro-González, M. How do Agaricomycetes shape their fruiting bodies? 1.
804 Morphological aspects of development. *Fungal Biology Reviews* **29**, 63–97 (2015).
- 805 7. Nagy, L. G., Kovács, G. M. & Krizsán, K. Complex multicellularity in fungi: evolutionary
806 convergence, single origin, or both? *Biol. Rev.* (2018). doi:10.1111/brv.12418
- 807 8. Bayry, J., Aïmanianda, V., Guijarro, J. I., Sunde, M. & Latgé, J. P. Hydrophobins-unique
808 fungal proteins. *PLoS Pathog.* **8**, (2012).
- 809 9. Plaza, D. F., Lin, C. W., van der Velden, N. S., Aebi, M. & Kunzler, M. Comparative
810 transcriptomics of the model mushroom *Coprinopsis cinerea* reveals tissue-specific
811 armories and a conserved circuitry for sexual development. *BMC Genomics* **15**, 492
812 (2014).
- 813 10. Buser, R., Lazar, Z., Käser, S., Kunzler, M. & Aebi, M. Identification, characterization, and
814 biosynthesis of a novel N-glycan modification in the fruiting body of the basidiomycete
815 *Coprinopsis cinerea*. *J. Biol. Chem.* **285**, 10715–10723 (2010).
- 816 11. Ohga, S., Cho, N.-S., Thurston, C. F. & Wood, D. A. Transcriptional regulation of laccase
817 and cellulase in relation to fruit body formation in the mycelium of *Lentinula edodes* on a
818 sawdust-based substrate. *Mycoscience* **41**, 149–153 (2000).
- 819 12. Konno, N. & Sakamoto, Y. An endo- β -1,6-glucanase involved in *Lentinula edodes*
820 fruiting body autolysis. *Appl. Microbiol. Biotechnol.* **91**, 1365–1373 (2011).
- 821 13. Sakamoto, Y. *et al.* *Lentinula edodes* tlg1 encodes a thaumatin-like protein that is

- 822 involved in lentinan degradation and fruiting body senescence. *Plant Physiol.* **141**, 793–
823 801 (2006).
- 824 14. Ohm, R. A., de Jong, J. F., de Bekker, C., Wösten, H. A. B. & Lugones, L. G.
825 Transcription factor genes of *Schizophyllum commune* involved in regulation of
826 mushroom formation. *Mol. Microbiol.* **81**, 1433–1445 (2011).
- 827 15. Corrochano, L. M. Fungal photoreceptors: sensory molecules for fungal development and
828 behaviour. *Photochem. Photobiol. Sci.* **6**, 725 (2007).
- 829 16. Sipos, G. *et al.* Genome expansion and lineage-specific genetic innovations in the forest
830 pathogenic fungi *Armillaria*. *Nat. Ecol. Evol.* **1**, 1931–1941 (2017).
- 831 17. Clémençon, H., Emmett, V. & Emmett, E. E. *Cytology and plectology of the*
832 *Hymenomycetes with 12 tables*. (Cramer in der Gebr.-Borntraeger-Verl.-Buchh, 2012).
- 833 18. Ernst, J. & Bar-Joseph, Z. STEM: A tool for the analysis of short time series gene
834 expression data. *BMC Bioinformatics* **7**, (2006).
- 835 19. Domazet-Lošo, T., Brajković, J. & Tautz, D. A phylostratigraphy approach to uncover the
836 genomic history of major adaptations in metazoan lineages. *Trends in Genetics* **23**, 533–
837 539 (2007).
- 838 20. Drost, H. G., Gabel, A., Grosse, I. & Quint, M. Evidence for active maintenance of
839 phylotranscriptomic hourglass patterns in animal and plant embryogenesis. *Mol. Biol.*
840 *Evol.* **32**, 1221–1231 (2015).
- 841 21. Gehrmann, T. *et al.* *Schizophyllum commune* has an extensive and functional alternative
842 splicing repertoire. *Sci. Rep.* **6**, (2016).
- 843 22. Xie, B.-B. *et al.* Deep RNA sequencing reveals a high frequency of alternative splicing
844 events in the fungus *Trichoderma longibrachiatum*. *BMC Genomics* **16**, 54 (2015).
- 845 23. Wang, B. *et al.* Survey of the transcriptome of *Aspergillus oryzae* via massively parallel
846 mRNA sequencing. *Nucleic Acids Res.* **38**, 5075–5087 (2010).
- 847 24. Gordon, S. P. *et al.* Widespread polycistronic transcripts in fungi revealed by single-
848 molecule mRNA sequencing. *PLoS One* **10**, (2015).
- 849 25. Enright, A. J., Van Dongen, S. & Ouzounis, C. A. An efficient algorithm for large-scale
850 detection of protein families. *Nucleic Acids Res.* **30**, 1575–1584 (2002).
- 851 26. Sakamoto, Y., Nakade, K. & Konno, N. Endo- β -1,3-Glucanase GLU1, from the fruiting
852 body of *Lentinula edodes*, belongs to a new glycoside hydrolase family. *Appl. Environ.*
853 *Microbiol.* **77**, 8350–8354 (2011).
- 854 27. Fukuda, K. *et al.* Purification and characterization of a novel exo-beta-1,3-1,6-glucanase
855 from the fruiting body of the edible mushroom *Enoki* (*Flammulina velutipes*). *Biosci.*
856 *Biotechnol. Biochem.* **72**, 3107–3113 (2008).
- 857 28. Zhou, Y., Zhang, W., Liu, Z., Wang, J. & Yuan, S. Purification, characterization and
858 synergism in autolysis of a group of 1,3- β -glucan hydrolases from the pilei of
859 *Coprinopsis cinerea* fruiting bodies. *Microbiol. (United Kingdom)* **161**, 1978–1989 (2015).
- 860 29. Szeto, C. Y., Leung, G. S. & Kwan, H. S. Le.MAPK and its interacting partner, Le.DRMIP,
861 in fruiting body development in *Lentinula edodes*. *Gene* **393**, 87–93 (2007).
- 862 30. Kersten, P. & Cullen, D. Copper radical oxidases and related extracellular
863 oxidoreductases of wood-decay Agaricomycetes. *Fungal Genet. Biol.* **72**, 124–130
864 (2014).
- 865 31. Rytioja, J. *et al.* Plant-Polysaccharide-Degrading Enzymes from Basidiomycetes.
866 *Microbiol. Mol. Biol. Rev.* **78**, 614–649 (2014).
- 867 32. Tovar-Herrera, O. E. *et al.* A novel expansin protein from the white-rot fungus
868 *Schizophyllum commune*. *PLoS One* **10**, (2015).
- 869 33. Lenfant, N. *et al.* A bioinformatics analysis of 3400 lytic polysaccharide oxidases from
870 family AA9. *Carbohydr. Res.* **448**, 166–174 (2017).
- 871 34. Temp, U. & Eggert, C. Novel interaction between laccase and cellobiose dehydrogenase
872 during pigment synthesis in the white rot fungus *Pycnoporus cinnabarinus*. *Appl. Environ.*

- 873 *Microbiol.* **65**, 389–395 (1999).
- 874 35. Osińska-Jaroszuk, M. *et al.* Complex biochemical analysis of fruiting bodies from newly
875 isolated polish *Flammulina velutipes* strains. *Polish J. Microbiol.* **65**, 295–305 (2016).
- 876 36. Ji, J. & Moore, D. Glycogen metabolism in relation to fruit body maturation in *Coprinus*
877 *cinereus*. *Mycol. Res.* **97**, 283–289 (1993).
- 878 37. Dranginis, A. M., Rauceo, J. M., Coronado, J. E. & Lipke, P. N. A Biochemical Guide to
879 Yeast Adhesins: Glycoproteins for Social and Antisocial Occasions. *Microbiol. Mol. Biol.*
880 *Rev.* **71**, 282–294 (2007).
- 881 38. Lugones, L. G. *et al.* Hydrophobins line air channels in fruiting bodies of *Schizophyllum*
882 *commune* and *Agaricus bisporus*. *Mycol. Res.* **103**, 635–640 (1999).
- 883 39. Gaderer, R., Bonazza, K. & Seidl-Seiboth, V. Cerato-platanins: A fungal protein family
884 with intriguing properties and application potential. *Applied Microbiology and*
885 *Biotechnology* **98**, 4795–4803 (2014).
- 886 40. Martin, F., Kohler, A., Murat, C., Veneault-Fourrey, C. & Hibbett, D. S. Unearthing the
887 roots of ectomycorrhizal symbioses. *Nat. Rev. Microbiol.* **14**, 760–773 (2016).
- 888 41. Stergiopoulos, I. & de Wit, P. J. G. M. Fungal Effector Proteins. *Annu. Rev. Phytopathol.*
889 **47**, 233–263 (2009).
- 890 42. Feldman, D., Kowbel, D. J., Glass, N. L., Yarden, O. & Hadar, Y. A role for small secreted
891 proteins (SSPs) in a saprophytic fungal lifestyle: Ligninolytic enzyme regulation in
892 *Pleurotus ostreatus*. *Sci. Rep.* **7**, (2017).
- 893 43. Wang, L., Tian, X., Gyawali, R. & Lin, X. Fungal adhesion protein guides community
894 behaviors and autoinduction in a paracrine manner. *Proc Natl Acad Sci U S A* **110**,
895 11571–11576 (2013).
- 896 44. Pellegrin, C., Morin, E., Martin, F. M. & Veneault-Fourrey, C. Comparative Analysis of
897 Secretomes from Ectomycorrhizal Fungi with an Emphasis on Small-Secreted Proteins.
898 *Front. Microbiol.* **6**, 1278 (2015).
- 899 45. Liu, T. B. & Xue, C. The ubiquitin-proteasome system and F-box proteins in pathogenic
900 fungi. *Mycobiology* **39**, 243–248 (2011).
- 901 46. Xu, G., Ma, H., Nei, M. & Kong, H. Evolution of F-box genes in plants: Different modes of
902 sequence divergence and their relationships with functional diversification. *Proc. Natl.*
903 *Acad. Sci.* **106**, 835–840 (2009).
- 904 47. Metzger, M. B., Pruneda, J. N., Klevit, R. E. & Weissman, A. M. RING-type E3 ligases:
905 Master manipulators of E2 ubiquitin-conjugating enzymes and ubiquitination. *Biochimica*
906 *et Biophysica Acta - Molecular Cell Research* **1843**, 47–60 (2014).
- 907 48. Chae, E., Tan, Q. K.-G., Hill, T. A. & Irish, V. F. An Arabidopsis F-box protein acts as a
908 transcriptional co-factor to regulate floral development. *Development* **135**, 1235–1245
909 (2008).
- 910 49. Pöggeler, S., Nowrousian, M., Teichert, I., Beier, A. & Kück, U. Fruiting-Body
911 Development in Ascomycetes. in *Physiology and Genetics* 1–56 (Springer International
912 Publishing, 2018). doi:10.1007/978-3-319-71740-1_1
- 913 50. Dharmasiri, N. *et al.* Plant Development Is Regulated by a Family of Auxin Receptor F
914 Box Proteins. *Dev. Cell* **9**, 109–119 (2005).
- 915 51. Pelkmans, J. F. *et al.* The transcriptional regulator c2h2 accelerates mushroom formation
916 in *Agaricus bisporus*. *Appl. Microbiol. Biotechnol.* **100**, 7151–7159 (2016).
- 917 52. Muraguchi, H. *et al.* Strand-specific RNA-seq analyses of fruiting body development in
918 *Coprinopsis cinerea*. *PLoS One* **10**, (2015).
- 919 53. Pelkmans, J. F. *et al.* Transcription factors of *schizophyllum commune* involved in
920 mushroom formation and modulation of vegetative growth. *Sci. Rep.* **7**, (2017).
- 921 54. Manning, G., Whyte, D. B., Martinez, R., Hunter, T. & Sudarsanam, S. The protein kinase
922 complement of the human genome. *Science* **298**, 1912–1934 (2002).
- 923 55. Kosti, I., Mandel-Gutfreund, Y., Glaser, F. & Horwitz, B. A. Comparative analysis of fungal

- 924 protein kinases and associated domains. *BMC Genomics* **11**, (2010).
- 925 56. Zhao, Z., Jin, Q., Xu, J. R. & Liu, H. Identification of a fungi-specific lineage of protein
926 kinases closely related to tyrosine kinases. *PLoS One* **9**, (2014).
- 927 57. Lehti-Shiu, M. D. & Shiu, S.-H. Diversity, classification and function of the plant protein
928 kinase superfamily. *Philos. Trans. R. Soc. B Biol. Sci.* **367**, 2619–2639 (2012).
- 929 58. Knoll, A. H. The Multiple Origins of Complex Multicellularity. *Earth Planet. Sci.* **39**, 217–
930 239 (2011).
- 931 59. Shiu, S. H. & Bleecker, a B. Plant receptor-like kinase gene family: diversity, function,
932 and signaling. *Sci. STKE* **2001**, re22 (2001).
- 933 60. Kunzler, M. Hitting the sweet spot-glycans as targets of fungal defense effector proteins.
934 *Molecules* **20**, 8144–8167 (2015).
- 935 61. Schubert, M. *et al.* Plasticity of the β -trefoil protein fold in the recognition and control of
936 invertebrate predators and parasites by a fungal defence system. *PLoS Pathog.* **8**,
937 (2012).
- 938 62. Cock, J. M. *et al.* The Ectocarpus genome and the independent evolution of
939 multicellularity in brown algae. *Nature* **465**, 617–621 (2010).
- 940 63. Sebe-Pedros, A., Degnan, B. M. & Ruiz-Trillo, I. The origin of Metazoa: a unicellular
941 perspective. *Nat Rev Genet* **18**, 498–512 (2017).
- 942 64. Nguyen, T. A. *et al.* Innovation and constraint leading to complex multicellularity in the
943 Ascomycota. *Nat Commun* **8**, 14444 (2017).
- 944 65. Granado, J. D., Kertesz-Chaloupková, K., Aebi, M. & Kües, U. Restriction enzyme-
945 mediated DNA integration in *Coprinus cinereus*. *Mol. Gen. Genet. MGG* **256**, 28–36
946 (1997).
- 947 66. Dons, J. J. M., De Vries, O. M. H. & Wessels, J. G. H. Characterization of the genome of
948 the basidiomycete *Schizophyllum commune*. *BBA Sect. Nucleic Acids Protein Synth.* **563**,
949 100–112 (1979).
- 950 67. Hibbett, D. S., Murakami, S. & Tsuneda, A. Hymenophore Development and Evolution in
951 *Lentinus*. *Mycologia* **85**, 428 (1993).
- 952 68. Fries, N. Basidiospore germination in some mycorrhiza-forming hymenomycetes. *Trans.*
953 *Br. Mycol. Soc.* **70**, 319–324 (1978).
- 954 69. Gnerre, S. *et al.* High-quality draft assemblies of mammalian genomes from massively
955 parallel sequence data. *Proc. Natl. Acad. Sci.* **108**, 1513–1518 (2011).
- 956 70. Martin, J. *et al.* Rnnotator: An automated de novo transcriptome assembly pipeline from
957 stranded RNA-Seq reads. *BMC Genomics* **11**, (2010).
- 958 71. Grigoriev, I. V *et al.* MycoCosm portal: Gearing up for 1000 fungal genomes. *Nucleic*
959 *Acids Res.* **42**, (2014).
- 960 72. Robinson, M. D., McCarthy, D. J. & Smyth, G. K. edgeR: a Bioconductor package for
961 differential expression analysis of digital gene expression data. *Bioinformatics* **26**, 139–
962 140 (2010).
- 963 73. Robinson, M. D. & Oshlack, A. A scaling normalization method for differential expression
964 analysis of RNA-seq data. *Genome Biol.* **11**, (2010).
- 965 74. Ritchie, M. E. *et al.* Limma powers differential expression analyses for RNA-sequencing
966 and microarray studies. *Nucleic Acids Res.* **43**, e47 (2015).
- 967 75. Dobin, A. *et al.* STAR: Ultrafast universal RNA-seq aligner. *Bioinformatics* **29**, 15–21
968 (2013).
- 969 76. Trapnell, C. *et al.* Transcript assembly and quantification by RNA-Seq reveals
970 unannotated transcripts and isoform switching during cell differentiation. *Nat. Biotechnol.*
971 **28**, 511–515 (2010).
- 972 77. Mancini, E., Iserte, J., Yanocsky, M. & Chernomoretz, A. ASpli: An integrative R package
973 for analysing alternative splicing using RNAseq - Semantic Scholar. (2017).
- 974 78. Torruella, G. *et al.* Phylogenomics Reveals Convergent Evolution of Lifestyles in Close

- 975 Relatives of Animals and Fungi. *Curr. Biol.* **25**, 2404–2410 (2015).
- 976 79. Darling, A. E., Carey, L. & Feng, W.-C. The Design, Implementation, and Evaluation of
977 mpiBLAST. in *ClusterWorld Conference & Expo and the 4th International Conference on*
978 *Linux Clusters: The HPC Revolution* (2003).
- 979 80. Lombard, V., Golaconda Ramulu, H., Drula, E., Coutinho, P. M. & Henrissat, B. The
980 carbohydrate-active enzymes database (CAZy) in 2013. *Nucleic Acids Res.* **42**, (2014).
- 981 81. Levasseur, A., Drula, E., Lombard, V., Coutinho, P. M. & Henrissat, B. Expansion of the
982 enzymatic repertoire of the CAZy database to integrate auxiliary redox enzymes.
983 *Biotechnol. Biofuels* **6**, (2013).
- 984 82. Ernst, J., Nau, G. J. & Bar-Joseph, Z. Clustering short time series gene expression data.
985 *Bioinformatics* **21**, (2005).
- 986 83. Pierleoni, A., Martelli, P. & Casadio, R. PredGPI: a GPI-anchor predictor. *BMC*
987 *Bioinformatics* **9**, 392 (2008).
- 988 84. Petersen, T. N., Brunak, S., Von Heijne, G. & Nielsen, H. SignalP 4.0: Discriminating
989 signal peptides from transmembrane regions. *Nature Methods* **8**, 785–786 (2011).
- 990 85. Horton, P. *et al.* WoLF PSORT: Protein localization predictor. *Nucleic Acids Res.* **35**,
991 (2007).
- 992 86. Melén, K., Krogh, A. & Von Heijne, G. Reliability measures for membrane protein
993 topology prediction algorithms. *J. Mol. Biol.* **327**, 735–744 (2003).
- 994 87. Shelest, E. Transcription Factors in Fungi: TFome Dynamics, Three Major Families, and
995 Dual-Specificity TFs. *Front. Genet.* **8**, 53 (2017).
- 996 88. Chen, L. *et al.* Genome Sequence of the Edible Cultivated Mushroom *Lentinula edodes*
997 (Shiitake) Reveals Insights into Lignocellulose Degradation. *PLoS One* **11**, e0160336
998 (2016).
- 999
- 1000

1001 Tables

1002 **Table 1 Conserved developmentally regulated (CAZyme) families and associated modules**

Family	Activity	Putative FCW role/substrate	Conservation	Reports of role in development	Expansion in Agaricomycetes
AA1_1	Laccase	crosslinking	5 (P.chr.)	Several reports	7.2x10 ⁻⁹⁰
AA3_1	Cellobiose dehydrogenase	chitin	5 (L.tig)	Temp&Eggert 1990	9.6x10 ⁻⁵⁶
AA3_2/3	Glucose oxidase, aryl alcohol oxidase	H ₂ O ₂ generation, light receptor?	6	This study	<10 ⁻³⁰⁰
AA5_1/2	Glyoxal oxidase, galactose oxidase	H ₂ O ₂ generation	6	This study	2.2x10 ⁻³
AA9	Lytic polysaccharide monooxygenase	chitin	6	This study	5.6x10 ⁻⁸⁶
CBM1	cellulose/chitin binding	chitin	5 (S.com.)	This study	n.s.
CBM12	Chitin binding	chitin	5 (P.chr.)	Sakamoto et al 2017	n.s.
CBM50	Chitin binding	chitin	5 (S.com.)	This study	1.7x10 ⁻⁵¹
CE4	chitooligosaccharide deacetylase	Chitin / chitosan	6	This study	6.4x10 ⁻¹¹
CE8	Pectin methylesterase	unknown	5 (C.cin.)	This study	n.s.
GH1_4	β-glucosidase	glucan	6	This study	n.s.
GH3_5	exo-β-1,3-glucanase	glucan	5 (A.ost.)	This study	n.s.
GH5_7	endo-β-1,4-mannanase	mannose	6	This study	4.9x10 ⁻⁷
GH5_15	endo-β-1,6-glucanase	glucan	5 (S.com.)	This study	2.7x10 ⁻⁸
GH5_49, GH5_9	endo-β-1,6-glucanase, exo-β-1,3-glucanase	glucan	6	Sakamoto et al 2017	1.3x10 ⁻³
GH6	Exo-β-1,4-glucanase, cellobiohydrolase	glucan	5 (S.com.)	This study	n.s.
GH12_1	endo-β-1,4-glucanase	glucan	5 (A.ost.)	This study	2.6x10 ⁻³

GH16	endo- β -1,3-1,4-glucanase	glucan	6	Sakamoto et al 2017	1.2×10^{-26}
GH16_2	endo- β -1,3-glucanase, endo- β -1,3-1,4-glucanase	glucan	5 (L.tig)	This study	1.2×10^{-26}
GH17	endo- β -1,3-glucanosyltransferase	glucan	6	This study	n.s.
GH18	chitinase	chitin	5 (L.tig)	This study	3.6×10^{-6}
GH18_5	chitinase	chitin	6	This study	3.6×10^{-6}
GH30_3	endo- β -1,6-glucosidase	glucan	6	Sakamoto et al 2017	2.7×10^{-14}
GH71	endo- β -1,3-glucanase	glucan	5 (P.chr.)	This study	1.6×10^{-7}
GH79_1	β -glucuronidase	unknown	4 (P.chr. S.com.)	This study	1.7×10^{-52}
GH92	α -1,3-mannosidase	mannose	5 (S.com.)	This study	2.1×10^{-18}
GH128	endo- β -1,3-glucanase	glucan	5 (P.chr.)	Sakamoto et al 2017, 2011	n.s.
GH152	β -1,3-glucanase, thaumatin	glucan	6	This study	2.0×10^{-18}
PL5	alginate lyase	?	6	This study	9.17×10^{-04}
PL14-like	alginate lyase-like	?	6	This study	8.5×10^{-19}
Expansins	cellulose/chitin loosening	chitin	6	Sipos et al 2017	1.5×10^{-94}
Kre9/Knh1	Glucan remodeling	glucan	6	Szeto et al 2007	1.5×10^{-05}

1003 Only families that are developmentally regulated in 5 or 6 species are shown (except GH79). Conservation of the
 1004 developmental regulation is given as the number of species in which a given family is developmentally regulated
 1005 followed by the name(s) of species in which there were no developmentally regulated members. Gene family
 1006 expansion in the Agaricomycetes was tested by a Fisher exact test, and considered significant at $P < 0.05$. For the
 1007 Kre9/Knh1 family, P-value refers to the overrepresentation of the corresponding InterPro domain.